ISSN 0018-1439, High Energy Chemistry, 2016, Vol. 50, No. 2, pp. 127–133. © Pleiades Publishing, Ltd., 2016.
Original Russian Text © E.I. Yudanova, V.R. Bogatyrenko, V.I. Krinichnyi, 2016, published in Khimiya Vysokikh Energii, 2016, Vol. 50, No. 2, pp. 132–138.

EPR Study of Spin Interactions in the Poly(3-dodecylthiophene) : Fullerene/Polyaniline : *p*-Toluenesulfonic Acid Composite

E. I. Yudanova, V. R. Bogatyrenko, and V. I. Krinichnyi
Institute of Problems of Chemical Physics, Russian Academy of Sciences,
pr. Akademika Semenova 1, Chernogolovka, Moscow oblast, 142432 Russia
e-mail: yudan@icp.ac.ru

Received February 2, 2015; in final form, July 1, 2015

Abstract—Magnetic, relaxation, and dynamic parameters of polarons $P_1^{\bullet+}$, trapped in *p*-toluenesulfonic acid-doped polyaniline, polarons $P_2^{\bullet+}$, and fullerene radical anions photoinduced in the poly(3-dodecylthiophene)/methanofullerene composite and in mixtures of these composites have been investigated using the EPR technique. It has been shown that spin charge carriers $P_2^{\bullet+}$ during diffusion along poly(3-dodecylthiophene) chains interact with $P_1^{\bullet+}$ trapped on adjacent polymer chains of polyaniline. The exchange interaction and spin relaxation in the ternary composites is determined by the activated hopping mobility of polarons $P_2^{\bullet+}$ and depends on the composition of the material.

Keywords: polyaniline, polythiophene, methanofullerene, polarons, exchange interactions, spin relaxation, photoinduced EPR

DOI: 10.1134/S0018143916010112

Possessing unique electronic properties, organic polymer semiconductors attract much attention of researchers in relation to their potential use as an active matrix of various molecular devices, such as field-effect transistors, light-emitting diodes, and solar cells [1]. These properties are mainly due to the fact that a charge in compounds of this class, unlike the case of conventional polymers, is transferred along localized states by topological distortions, namely solitons, polarons, and bipolarons. The polaron spin of $S = 1/2$ determines the dependence of the effective mobility of such charge carriers upon the mutual orientation of their spins, which can be altered by external or internal magnetic fields. The spin state of the initial polymer matrix can be changed by introducing one or more spin ensembles into the matrix. Thus, the introduction of a certain amount of a galvinoxyl radical into a photovoltaic organic polymer : fullerene system made it possible to improve the efficiency of conversion of light into electrical energy [2].

To obtain a multispin system, we used two polymeric matrices. In [3], it was shown that polyaniline fully doped with *para*-toluenesulfonic acid (PANI : *p*TSA) can be successfully used as the main spin reservoir. According to generally adopted concepts, doping results in the formation of highly conductive crystalline domains in the amorphous phase of this polymer [4, 5] and the dynamics of charge transport in PANI blends with other polymers is different. For example, Wessling et al. [5] showed that the efficiency of charge transport in PANI : *p*TSA is substantially enhanced by its dispersing in poly(methyl methacrylate) (PMMA) to have an optimum PANI : *p*TSA content (7% and 17%) of the resulting PANI : *p*TSA/PMMA composite. A detailed study of PANI using a multifrequency EPR technique [6] allowed us to conclude that the relaxation and dynamic parameters of the spin carriers are dependent significantly on the crystallinity and ordering of their microenvironment, the composite morphology, and the molecular structure of the dopant introduced into the polymer. Polarons generated by doping PANI are characterized by high stability of their basic parameters owing to the conformational stability of the spin state of the majority of polyanilines. Studies of PANI : *p*TSA revealed increased accessibility of polarons for foreign spins, in particular, molecular oxygen diradical [7, 8]. The exchange interaction of both spin ensembles in that case is determined by the properties of the PANI polymer matrix and the precession frequency of the polaron spins. It is for this reason that we choose the doped polymer PANI : *p*TSA as the polymer matrix. The second component to be blended with PANI was the photovoltaic polymer : fullerene composite based on poly(3-dodecylthiophene) (P3DDT) and the fullerene derivative PCBM (6,6-phenyl-C_{61}-butanoic acid methyl ester), P3DDT : PCBM. In previous studies [9–11] we have shown that irradiation of P3DDT : PCBM space het-

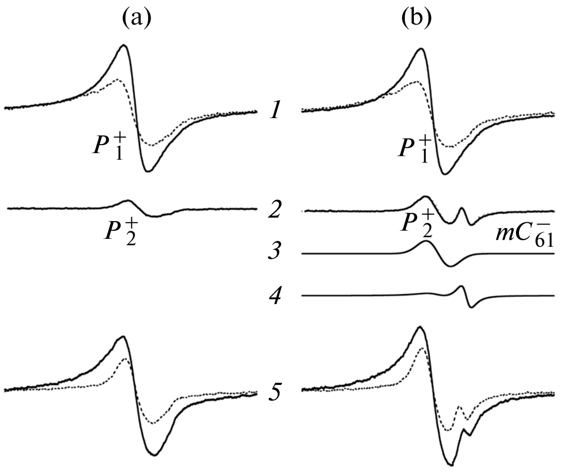

Fig. 1. EPR spectra recorded in the (a) dark and (b) light at $T = 77$ K for (*1*) the PANI : *p*TSA/P3DDT composite, the dashed curve refers to $P_1^{\bullet+}$ polarons; (*2*) the P3DDT : PCBM composite, containing the contributions of (*3*) $P_2^{\bullet+}$ polarons and (*4*) $mC_{61}^{\bullet-}$; and (*5*) the PPP composites (dashed curve) PPP1 and (solid curve) PPP2. The dotted curve in spectrum *2* shows the spectrum calculated assuming the linewidths of polarons and fullerene radical anions to be $\Delta B_{pp}^{P} = 2.93$ G and $\Delta B_{pp}^{mF} = 1.23$ G, respectively, with *g*-factors of $g_{iso}^{P} = 2.001552$ and $g_{iso}^{mF} = 1.99988$ at a $[P_2^{\bullet+}]/[mC_{61}^{\bullet-}]$ concentration ratio of 6.56.

erojunctions with photons of optical range generates in them polarons—both freely diffusing throughout the polymer matrix and trapped in the crystalline or the amorphous phase of the polymer—and methanofullerene radical anions pseudo-rotating between polymer chains. In this paper, we present the results of an EPR study of the magnetic, relaxation, and dynamic parameters of spin carriers trapped in PANI : *p*TSA/P3DDT : PCBM composites with different polymer ratios over a wide temperature range. The results have been rationalized in terms of exchange interaction of spin ensembles trapped and photoinduced in these systems.

EXPERIMENTAL

We used doped polyaniline PANI : *p*TSA, manufactured by Ormecon, with a doping level of $y = [S]/[N] = 0.5$, synthesized according to a procedure specified in [12]. Commercial soluble regioregular P3DDT (Aldrich) and PCBM available from Solenne BV were used for preparing the corresponding P3DDT: PCBM photovoltaic space heterojunctions. P3DDT and PCBM in a 1 : 1 ratio were dissolved in chloroform to have a concentration of 1 wt %, and the solution was cast layer by layer onto a ceramic substrate and dried. Two layers were sequentially applied onto each side of the substrate. As a result, a P3DDT : PCBM composite film of a 4 × 8 mm^2 size and a ~0.1 mm thickness was formed. This polymer : fullerene composite was studied as a reference photovoltaic system illuminated with white light in a nitrogen atmosphere. Then PANI : *p*TSA powders were mixed with a P3DDT and PCBM solution in chloroform so that the PANI content of the mixture reached 7% (PANI-07/P3DDT) or 17% (PANI-17/P3DDT) of the total polymer mass. The resulting solutions were applied dropwise (drop size of $V = 5$ μL) onto a ceramic substrate, with two drops being gradually applied with drying on each side of the ceramic substrate. For a comparative study of the mutual influence of spins on each other in different spin reservoirs, the following samples were prepared: a P3DDT : PCBM composite; the PANI : *p*TSA doped polymer; a PANI/PCBM blend (P1); PANI-07/P3DDT (PP1) and PANI- 17/P3DDT (PP2) binary composites; and PANI 07/P3DDT/PCBM (PPP1) and PANI-17/P3DDT/PCBM (PPP2) ternary composites with PANI contents of 7 and 17%, respectively.

EPR measurements were made on a PS100X radiospectrometer (3 cm, 9.7 GHz) equipped with a VRT thermal attachment manufactured by the Special Design Bureau at the Zelinsky Institute of Organic Chemistry (Russia). The measurements were performed in a nitrogen atmosphere at a polarizing-field modulation frequency of 100 kHz. The EPR spectra of polymer : fullerene composites were recorded at 77 K by immersing them in a quartz cell filled with liquid nitrogen. The samples were illuminated directly in the spectrometer cavity with white light from an LP5W-80F320CW source (5 W, 320 lm, 5500 K). The signal-to-noise ratio of the EPR spectra was increased by accumulating signals with multiple scanning. Paramagnetic susceptibility was determined by double integration of individual lines of the EPR spectra recorded well away from their saturation conditions. All relaxation parameters of charge carriers were determined separately using the method of continuous wave saturation of EPR spectra [8]. The processing and simulation of the EPR spectra were performed using the program OriginLab.

RESULTS AND DISCUSSION

Figure 1 shows EPR spectra of the paramagnetic centers $P_1^{\bullet+}$, $P_2^{\bullet+}$, and $mC_{61}^{\bullet-}$, trapped and photoinduced in the PANI : *p*TSA/P3DDT, P3DDT : PCBM, PPP1, and PPP2 composites at $T = 77$ K. From Fig. 1 it is seen that the EPR spectrum of PANI : *p*TSA is a singlet line due to positively charged $P_1^{\bullet+}$, polarons trapped on chains of the polymer matrix. The concentration of $P_1^{\bullet+}$ polarons in the PANI : *p*TSA/P3DDT composites increases with an increase in the relative PANI content and does not depend on illumination. However, the concentration and composition of paramagnetic centers $P_2^{\bullet+}$ and $mC_{61}^{\bullet-}$ in the P3DDT : PCBM composite change during illumination. Spectrum *2* shown in Fig. 1b for this composite consists largely of Lorentzain contributions *3* of $P_2^{\bullet+}$, polarons captured by spin traps and doublets *4* due to mobile radical pairs $P_2^{\bullet+}$–$mC_{61}^{\bullet-}$, positively charged $P_2^{\bullet+}$, polarons diffusing freely along chains of the polymer matrix, and negatively charged methanofullerene radical ions rotating between the polymer chains. Analysis of photoinduced changes in the EPR spectra of the composites and deconvolution of the spectra into individual components made it possible to calculate individual contributions of all the spin carriers to the EPR spectrum in a way similar to that used in the study of other polymer composites [11, 13–15]. Effective *g*-factors of all of the spin carriers generated at $T = 77$ K are shown in Table 1. An analysis showed that the field position of the $P_1^{\bullet+}$ polaron spectra slightly depends on temperature over the entire temperature range, a behavior that is typical of paramagnetic centers in highly conductive crystalline compounds [16, 17]. The isotropic *g*-factor of the $mC_{61}^{\bullet-}$ radical anion behaves in the same manner. Figure 2 shows that the *g*-factor of $P_2^{\bullet+}$, polarons trapped on P3DDT chains begins to depend upon temperature in the ternary composites PPP1 and PPP2. Taking into account the direct dependence of the *g*-factor on spin–orbit coupling (characterized by a constant λ) and its inverse dependence on the spin excitation energy $n \rightarrow \pi^*$ ($\Delta E_{n\pi^*}$) and $\sigma \rightarrow \pi^*$ ($\Delta E_{\sigma\pi^*}$), we can conclude that the spin–orbit coupling and the spin state noticeably change in the final PPP composites, with the changes being manifested to the greatest extent in the PPP1composite. As in the case of other poly(3-alkylthiophene)s [18, 19], this can be explained by the appearance of joint harmonic libration of polymer matrix chains with polarons stabilized on them, which modulates the charge transport integral. This macromolecular dynamics should lead to the following temperature dependence of the effective *g*-factor:

$$g_{\text{iso}}(T) = g_0 + \frac{A}{\omega_1}\coth\left(\frac{\hbar\omega_1}{2k_{\text{B}}T}\right), \qquad (1)$$

where g_0 and A are constants, $\hbar = h/2\pi$ is Planck's constant, $\omega_1 = \omega_0\exp(-E_1/k_{\text{B}}T)$ is the libration frequency, E_1 is the energy required to activate the libration movement, and k_{B} is Boltzmann's constant. Figure 2 shows the relationships calculated using Eq. (1) with $g_0 = 2.00331$ and $E_1 = 0.0268$ eV or $g_0 = 2.00532$ and $E_1 = 0.0046$ eV for PPP2 or PPP1, respectively. These values are well below the activation energy of libration oscillations in radical ion salts, which is ~0.1 eV [20], suggesting a lower crystallinity of the polymer matrices of the PANI : *p*TSA/P3DDT : PCBM composites.

Table 1. Effective values of *g*-factors (g_{iso}) of paramagnetic centers $P_1^{\bullet+}$, $P_2^{\bullet+}$ and $mC_{61}^{\bullet-}$ trapped in the initial P3DDT : PCBM composite and the PPP1 and PPP2 composites at $T = 77$ K

g-factor	P3DDT : PCBM	PPP1	PPP2
$g_{\text{iso}}^{\text{P1}}$	–	2.002_{63}	2.002_{90}
$g_{\text{iso}}^{\text{P2}}$	2.001_{55}	2.001_{68}	2.002_{07}
$g_{\text{iso}}^{\text{C61}}$	1.999_{88}	2.000_{43}	2.000_{37}

EPR Linewidth of Polarons

Figures 3a and 3b show the temperature dependence of effective absorption linewidth ΔB_{pp} and spin susceptibility χ_1 for $P_1^{\bullet+}$ polarons trapped in initial PANI : *p*TSA, the P1 sample, the PP1 and PP2 polymer blends, and the PPP1 and PPP2 ternary composites. In the latter two cases, the signals were recorded in the dark and under illumination. From Fig. 3a it is seen that an increase in the temperature results in a monotonic decrease in linewidth ΔB_{pp} of $P_1^{\bullet+}$ polarons in the initial samples of PANI : *p*TSA. For the P1 sample and the PP1 and PP2 composites consisting of a mixture of polymers, the change in the $P_1^{\bullet+}$ EPR linewidth with temperature is weaker as compared with the initial PANI : *p*TSA sample. Note that the linewidth for the PP1 or PP2 composite varies in the range of $\Delta B_{\text{pp}} = 3.2$–$4.0$ or 2.5–3.2 G, respectively. The linewidth for the P1 sample depends on temperature in a similar manner and varies in the range of $\Delta B_{\text{pp}} = 1.9$–$3.0$ G. Obviously, the EPR linewidth of different samples depends on the composition of the composites. The effect of PCBM on polaron $P_1^{\bullet+}$ in the P1 composite is similar to that of the second polymer in the PP1 and PP2 blends, with a stepwise change in the linewidth at a temperature of 150 K being observed in all

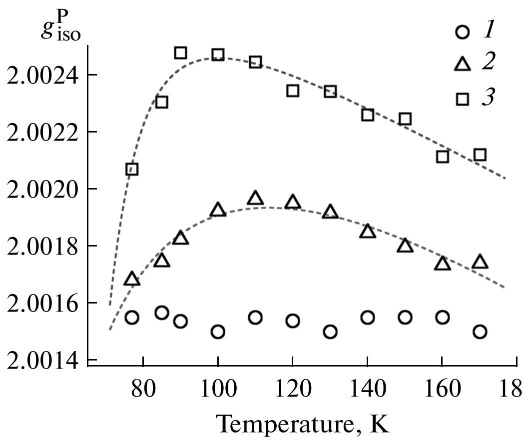

Fig. 2. Temperature dependence of $g_{\text{iso}}^{\text{P}}$ of $P_2^{\bullet+}$ polarons in the(*1*) P3DDT : PCBM, (*2*) PPP1, and (*3*) PPP2 composites.

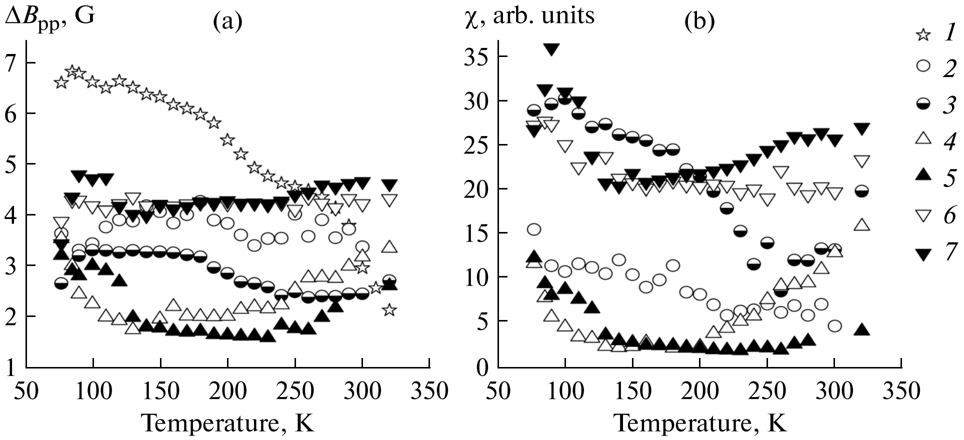

Fig. 3. Temperature dependence of (a) ΔB_{pp} and (b) χ_1 of $P_1^{\bullet+}$, polarons trapped in (*1*) the initial PANI : *p*TSA polymer; (*2*) PP1 and (*3*) PP2 composites; and (*4, 5*) PPP1 and (*6, 7*) PPP2 composites in the (*4, 6*) dark and (*5, 7*) light.

of the samples, a behavior that can be due to conformational rearrangements in PANI at this temperature. There are significant differences in the temperature dependence of ΔB_{pp} between the ternary PPP systems, which are especially noticeable for the PPP1sample. Compared with the PP1 binary composite, the ΔB_{pp} value in the ternary composite PPP1 decreased from 4.0 to 1.8 G, and ΔB_{pp} in the PP2 and PPP2 composites increased from 3.3 to 4.3 G, respectively. The temperature dependence curves of ΔB_{pp} for PPP1 acquired the U-shaped pattern, and illumination resulted in the appearance of an additional, small maximum at $T = 100$ K. The $P_1^{\bullet+}$ polaron linewidth for the PPP2 composite remains almost unchanged by temperature, but illumination of its samples gives rise to a small peak at $T = 100$ K. It is obvious that the extremum appearing on the ΔB_{pp} curves at $T = 100$ K is associated with the formation of new, photoinduced spin states in P3DDT : PCBM. Thus, the composition of the polymer composites has a significant effect on linewidth ΔB_{pp} and its temperature dependence for $P_1^{\bullet+}$ trapped by PANI chains.

Figures 4a and 4b respectively show the temperature dependences of ΔB_{pp} and spin susceptibility χ_2 for $P_2^{\bullet+}$, polarons photoinduced in P3DDT : PCBM space heterojunctions in the test composites. The EPR linewidth of $P_2^{\bullet+}$ polarons in the P3DDT : PCBM composite is almost independent of temperature, unlike the case of $P_1^{\bullet+}$ polarons in initial PANI : *p*TSA. The introduction of conducting PANI into this subsystem changes the slope of the temperature dependence of ΔB_{pp} for $P_2^{\bullet+}$ with the curves for PPP1 and PPP2 composites almost coinciding. However, an extremum with a critical point $T_c \approx 110$ K associated with the photoinitiation of mobile $P_2^{\bullet+}$ polarons and fullerene radical anions $mC_{61}^{\bullet-}$ appears on the ΔB_{pp} temperature dependence curve for $P_2^{\bullet+}$, polarons as a result of illumination. A similar temperature extremum of ΔB_{pp} was observed in the EPR study of exchange interactions of polarons with oxygen diradicals diffusing in PANI fully doped with hydrochloric acid [21] or *p*TSA [22]. In the papers cited, this effect was attributed to the exchange interaction between oxygen and polarons. The interaction is described by an exchange integral or spin exchange constant J_{ex}. Polarons move by hopping on the polymer chain at a speed ω_{hop} through an energy barrier E_b. In our composites, a broadening agent for $P_1^{\bullet+}$ and $P_2^{\bullet+}$ polarons can be mobile radical pairs photoinduced in the ternary systems. By spin collisions, the EPR linewidth should be broadened as follows [23] :

$$\delta(\Delta\omega) = p\omega_{hop}n_P = \frac{1}{2}\omega_{hop}n_P\left(\frac{\alpha^2}{1+\alpha^2}\right), \qquad (2)$$

where p is the probability of inversion during the collision of both spins, $\omega_{hop} = \omega_{hop}^0 \exp(-E_b/k_BT)$, E_b is the activation energy of polaron mobility for moving along the polymer chain, n_P is the number of $P_2^{\bullet+}$, polarons per PANI monomer unit, and $\alpha = (3/2)2\pi J_{ex}/\hbar\omega_{hop}$. It is known [23] that the linewidth change is described by expression $(\delta\Delta\omega) \sim 1/2n_P\omega_{hop}$ in the case of strong exchange and the inverse relationship $(\delta\Delta\omega) \sim n_P/\omega_{hop}(J_{ex}/\hbar)^2$ in the case of weak exchange. If these conditions are realized in the spin system at $T \le T_c$ and $T \ge T_c$, respectively, the temperature dependence of the linewidth will be nonmonotonic with a characteristic point T_c. It is these extremums at $T_c = 100$–110 K that are observed for $P_1^{\bullet+}$ and $P_2^{\bullet+}$ polarons photogenerated by white light in the PPP1 and PPP2 composites. Figure 4a shows curves calculated by Eq. (2) with acti-

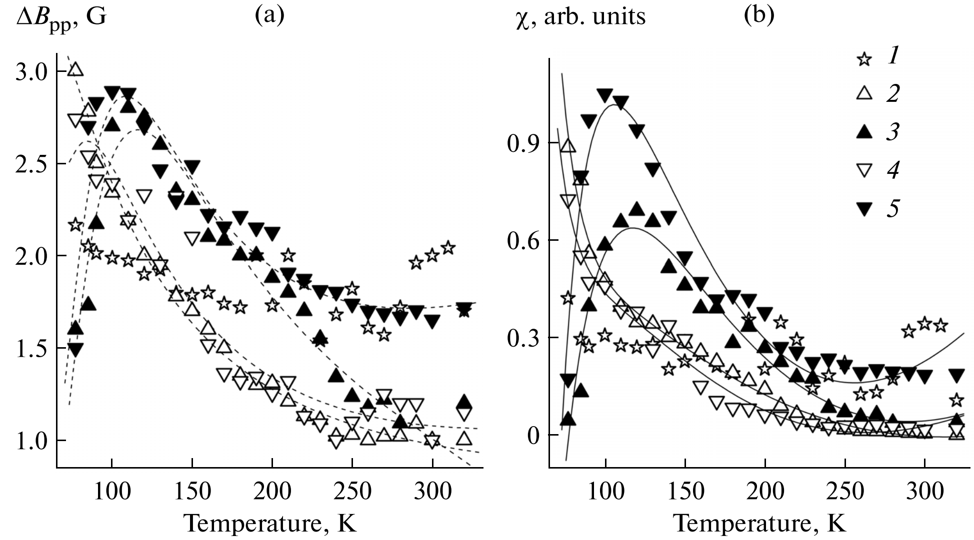

Fig. 4. Temperature dependence of (a) ΔB_{pp} and (b) χ_2 of $P_2^{\bullet+}$, polarons in (*1*) the initial P3DDT : PCBM composite and the (*2*, *3*) PPP1 and (*4*, *5*) PPP2 composites in the dark (*2*, *4*) and (*3*, *5*) light. The dashed curves refer to theoretical relations calculated by Eqs. (a) (3) and (b) (2) with the relevant values of E_{b} and J_{af}.

vation energies E_{b} presented in Table 2. The activation energy of the motion of $P_2^{\bullet+}$ polaron along the P3DDT chain is determined by both the PANI content in the PPP1 or PPP2 composite and the effect of light photons on the composite. Thus, it can be concluded that E_{b} is considerably increased by increasing the relative amount of PANI in the composite and by exposure to light.

Paramagnetic Susceptibility of Polarons

Figure 3b shows the temperature dependence of spin susceptibility χ_1 for $P_1^{\bullet+}$ polarons trapped in the test composites. As the temperature increases, χ_1 in the mixtures of two subsystems PP1, PP2, and P1 monotonically decreases. For the PPP2 ternary composite, the temperature dependences of χ_1 in the dark and under illumination are close to those obtained for the binary composite PP2. However, the temperature dependence curves of χ_1 of the ternary composite PPP1 take the U-shaped form with a minimum at $T =$ 150 K. Note that the temperature dependences of the $P_1^{\bullet+}$ linewidth undergo similar changes at a temperature about 150 K, which are presumably due to structural rearrangements in PANI at this temperature. The temperature dependence curves shown in Fig. 4b for χ_2 of $P_2^{\bullet+}$ polarons in the initial P3DDT : PCBM composite and the ternary composites are close to one another, with χ_2 decreasing monotonically with an increase in temperature. Irradiation with light results in extremums at $T = 110$ K—similar to the changes in linewidth ΔB_{pp} for $P_2^{\bullet+}$, —on the temperature dependence curves of χ_2 for $P_2^{\bullet+}$ polarons in the PPP1 and PPP2 composites; we associate the extremums primarily with the appearance of mobile pairs of $P_2^{\bullet+}$ polarons and $m\mathrm{C}_{61}^{\bullet-}$ fullerene radical anions. As has been already noted, an increase in number of spin carriers in the ternary systems leads to exchange interactions between them. The pattern of the temperature dependence of susceptibility χ gives important information about mobile and localized spins in the system and on

Table 2. Values of J_{af} determined using Eq. (3) for $P_2^{\bullet+}$ polarons, $E_{\mathrm{b}}^{|}$ determined using Eq. (2) for $P_2^{\bullet+}$ polarons and $m\mathrm{C}_{61}^{\bullet-}$ methanofullerene radical anions, and $E_{\mathrm{b}}^{|}$ determined using Eq. (4) for the $m\mathrm{C}_{61}^{\bullet-}$ methanofullerene radical anions

Parameter	P3DDT	PPP1 dark	PPP1 light	PPP2 dark	PPP2 light
E_{b} ($P_2^{\bullet+}$), eV	–	0.0080	0.0158	0.0122	0.0177
J_{af} ($P_2^{\bullet+}$), eV	–	0.0072	0.0041	0.0063	0.0012
E_{b} ($m\mathrm{C}_{61}^{\bullet-}$), eV	0.0003	–	0.0015	–	0.0005
$E_{\mathrm{b}}^{|}$ ($m\mathrm{C}_{61}^{\bullet-}$), eV	0.0011	–	0.0075	–	0.0111

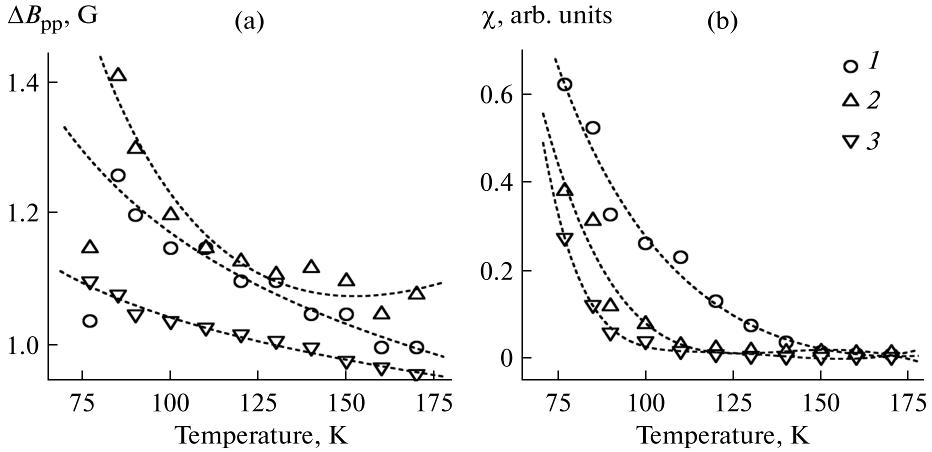

Fig. 5. Temperature dependence of (a) $\Delta B_{\rm pp}$ and (b) χ of the PCBM methanofullerene radical anion photogenerated in the (*1*) P3DDT : PCBM, (*2*) PPP1, and (*3*) PPP2 composites. The dashed curves in Figs. 5a and 5b present the results of calculation by Eqs. (2) and (4), respectively, with the values of $E_{\rm b}$ and $E_{\rm b}^{|}$, as given in Table 2.

their ability to interact. The susceptibility for noninteracting electrons in disordered regions obeys the Curie law $\chi_C \infty 1/T$, whereas the polarons delocalized in conducting ordered crystallites exhibit temperature-independent behavior according to the Pauli law χ_P. However, most of the spins in polyaniline and other conductive polymers are localized and exchange and dipole interactions occur between them. These lead to the appearance in the general equation for paramagnetic susceptibility of the corresponding term $\chi_{\rm ST}$ relating to the antiferromagnetic coupling of spins in the singlet and triplet states [24]:

$$\chi(T) = \chi_{\rm P} + \chi_{\rm C} + \chi_{\rm ST} = N_{\rm A}\mu_{\rm eff}^2 n(\varepsilon_{\rm F}) + \frac{N\mu_{\rm eff}^2}{3k_{\rm B}T} + \frac{k_1}{T}\left[\frac{\exp(-J_{\rm af}/k_{\rm B}T)}{1+3\exp(-J_{\rm af}/k_{\rm B}T)}\right]^2, \quad (3)$$

where $N_{\rm A}$ is Avogadro's number, $\mu_{\rm eff} = \mu_{\rm B} g\sqrt{S(S+1)}$ is the effective magneton, $\mu_{\rm B}$ is the Bohr magneton, $n(\varepsilon_{\rm F})$ is the density of states for both spin orientations at the Fermi level $\varepsilon_{\rm F}$, $N\mu_{\rm eff}^2/3k_{\rm B} = C$ is the Curie constant, k_1 is a constant, and $J_{\rm af}$ is the antiferromagnetic coupling integral. Figure 4b depicts theoretical curves calculated by Eq. (3) with the relevant values of $J_{\rm af}$ given in Table 2. The experimental and theoretical curves calculated in this model agree well with one another. The values of $J_{\rm af}$ obtained for $P_2^{\bullet+}$ polarons in the PPP1 and PPP2 composites in the dark are close in order of magnitude. However, $J_{\rm af}$ significantly decreases when these composites are illuminated with white light. This decrease suggests enhancement of the exchange interaction between the charge carriers of both spin ensembles, with the most significant change occurring in the PPP2 composite. It should be noted that this spin–spin coupling mechanism differs from that in a composite with microcrystalline PANI [3], presumably, because of the difference in morphology between these compounds.

EPR Parameters of Fullerene Radical Anions

Figure 5 shows temperature dependence curves for $\Delta B_{\rm pp}$ and susceptibility χ of fullerene radical anions $m{\rm C}_{61}^{\bullet-}$, photogenerated in the P3DDT : PCBM, PPP1, and PPP2 complexes. It is seen that during heating of the P3DDT : PCBM sample, the linewidth of the $m{\rm C}_{61}^{\bullet-}$ radical anion first increases and then decreases in the same manner as described in [7, 10]. The pattern of the temperature dependence of $\Delta B_{\rm pp}$ in the PPP1 composite varies in a similar fashion and is somewhat different in the case of PPP2. Spin susceptibility χ of the $m{\rm C}_{61}^{\bullet-}$ radical anion in the both composites decreases with an increase in temperature (Fig. 5b), a change that is due to enhancement of recombination of polarons and fullerene radical anions of the $P_2^{\bullet+}$–$m{\rm C}_{61}^{\bullet-}$ radical pair. During the formation and recombination of $P_2^{\bullet+}$ and $m{\rm C}_{61}^{\bullet-}$, the net spin susceptibility of both carriers is recorded by EPR, which is characterized by the inverse relation to probability p of such recombination [25]. In this case, the effective spin susceptibility of the quasi-pair can be written as:

$$\chi = \chi_0 \frac{2(1+\alpha^2)}{\alpha^2}\exp\left(\frac{E_{\rm b}^{|}}{k_{\rm B}T}\right), \quad (4)$$

where $E_{\rm b}^{|}$ is the thermal activation energy of movement of charge carriers along the polymer chain. Figure 5b presents the theoretical dependence calculated by Eq. (4) with the $E_{\rm b}^{|}$, values given in Table 2; from these data it follows that the value of E_b determined for the $\mathrm{P}_2^{\bullet+}$ polaron significantly exceeds $E_\mathrm{b}^{|}$ for the methanofullerene radical anion $m\mathrm{C}_{61}^{\bullet-}$.

CONCLUSIONS

In the PANI : *p*TSA/P3DDT : PCBM multispin polymer composite, there is overlap of the wave functions of polarons trapped on neighboring chains of the PANI and P3DDT polymer matrices, leading to their exchange interaction. Comparison of the temperature dependences of the EPR parameters for $\mathrm{P}_1^{\bullet+}$ and $\mathrm{P}_2^{\bullet+}$ polarons in the test composites leads to the conclusion that spin–spin coupling of charge carriers in the PPP ternary composites has a significant effect on the relaxation characteristics of $\mathrm{P}_1^{\bullet+}$ and $\mathrm{P}_2^{\bullet+}$ polarons. It has been shown that this coupling is determined by the structure, composition, and morphology of the both polymer matrices, as well as by the relaxation and dynamic parameters of all of the spin ensembles. Photogeneration of spin pairs creates an additional channel for controlling the electronic properties of the composite made of different polymer spin subsystems. The revealed correlations between the electronic and structural parameters of these systems can be used for optimizing the electronic properties and controlling of the next-generation organic electronic devices.

ACKNOWLEDGMENTS

This work was supported by the Russian Foundation for Basic Research, project no. 12-03-00148a, and the Russian Academy of Sciences under Presidium program no. 1, grant no. 15-039.

REFERENCES

1. Heeger, A.J., Sariciftci, N.S., and Namdas, E.B., *Semiconducting and Metallic Polymers*, London: Oxford University Press, 2010.
2. Zhang, Y., Gautam, B.R., Basel, T.P., Mascaro, D.J., and Vardeny, Z.V., *Synth. Met.*, 2013, vol. 173, no. 1, p. 2.
3. Krinichnyi, V.I., Yudanova, E.I., and Wessling, B., *Synth. Met.*, 2013, vol. 179, p. 67.
4. Wang, Z.H. and Scherr, E.M., MacDiarmid, A.G., and Epstein, A.J, *Phys. Rev. B*, 1992, vol. 45, no. 8, p. 4190.
5. Wessling, B., Srinivasan, D., Rangarajan, G., Mietzner, T., and Lennartz, W., *Eur. Phys. J. E*, 2000, vol. 2, no. 3, p. 207.
6. Krinichnyi, V.I., *Appl. Phys. Rev.*, 2014, vol. 1, no. 2, p. 021305.
7. Krinichnyi, V.I., Tokarev, S.V., Roth, H.K., Schrodner, M., and Wessling, B., *Synth. Met.*, 2006, vol. 156, nos. 21–24, p. 1368.
8. Krinichnyi, V.I., Roth, H.K., Schrodner, M., and Wessling, B., *Polymer*, 2006, vol. 47, no. 21, p. 7460.
9. Krinichnyi, V.I., *Acta Mater.*, 2008, vol. 56, no. 7, p. 1427.
10. Krinichnyi, V.I. and Balakai, A.A., *Appl. Magn. Reson.*, 2010, vol. 39, no. 3, p. 319.
11. Krinichnyi, V.I., Yudanova, E.I., and Spitsina, N.G., *J. Phys. Chem. C,* 2010, vol. 114, no. 39, p. 16756.
12. Lux, F., Hinrichsen, G., Krinichnyi, V.I., Nazarova, I.B., Chemerisov, S.D., and Pohl, M.M., *Synth. Met.*, 1993, vol. 55, no. 1, p. 347.
13. Takeda, K., Hikita, H., Kimura, Y., Yokomichi, H., and Morigaki, K., *Jpn. J. Appl. Phys.*, 1998, vol. 37, no. 12A, p. 1730.
14. Yanilkin, V.V., Nastapova, N.V., Morozov, V.I., Gubskaya, V.P., Sibgatullina, F.G., Berezhnaya, L.S., and Nuretdinov, I.A., *Russ. J. Electrochem.*, 2007, vol. 43, no. 2, p. 184.
15. Poluektov, O.G., Filippone, S., Martin, N., Sperlich, A., Deibel, C., and Dyakonov, V., *J. Phys. Chem. B*, 2010, vol. 114, no. 45, p. 14426.
16. Krinichnyi, V.I., *Izv. Akad Nauk, Ser. Khim.*, 2000, no. 2, p. 205.
17. Krinichnyi, V.I., *Synth. Met.*, 2000, vol. 108, no. 3, p. 173.
18. Krinichnyi, V.I. and Roth, H.K., *Appl. Magn. Reson.*, 2004, vol. 26, p. 395.
19. Krinichnyi, V.I. and Yudanova, E.I., *Sol. Energy Mater. Sol. Cells*, 2011, vol. 95, p. 2302.
20. Williams, J.M., Ferraro, J.R., Thorn, R.J., Carlson, K.D., Geiser, U., Wang, H.H., Kini, A.M., and Whangboo, M.-H., in *Organic Superconductors (Including Fullerenes): Synthesis, Structure, Properties, and Theory*, Grimes, R.N., Ed., Upper Saddle River, NJ: Prentice-Hall, 1992
21. Houze, E. and Nechtschein, M., *Phys. Rev. B*, 1996, vol. 53, no. 21, p. 14309.
22. Krinichnyi, V.I., Tokarev, S.V., Roth, H.K., Schrodner, M., and Wessling, B., *Synth. Met.*, 2005, vol. 152, nos. 1–3, p. 165.
23. Molin, Y.N., Salikhov, K.M., and Zamaraev, K.I., *Spin Exchange*, Berlin: Springer, 1980.
24. Vonsovskii, S.V., *Magnetizm, Magnitnye svoistva dia-, para-, ferro-, antiferro- i ferrimagnetikov* (Magnetism: Magnetic Properties of Dia-, Para- Ferro- and Antiferromagnetics), Moscow: Nauka, 1971.
25. Nelson, J., *Phys. Rev. B*, 2003, vol. 67, no. 15, p. 155209.

Translated by S. Zatonsky